Melting Behaviors of Nanocrystalline Ag

Shifang Xiao,*,† Wangyu Hu,*,†,‡ and Jianyu Yang†

Department of Applied Physics, Hunan University, Changsha 410082, China, and Material Science and Engineering College, Hunan University, Changsha 410082, China

Received: August 13, 2005

In the atomic scale, the melting behaviors of nanocrystalline Ag with mean grain size ranging from 3.03 to 12.12 nm have been investigated with molecular dynamics simulations, and a method to determine the melting temperatures of the infinite polycrystalline nanostructured materials is presented. It is found that the melting in nanostructured polycrystals starts from their grain boundaries, and the relative numbers of the three typical bonded pairs, (1551), (1431), and (1541), existing in the liquid phase, increase rapidly with the evolvement of melting. The melting temperatures of nanocrystalline Ag decrease with decreasing mean grain size, and it can be estimated from the size-dependent melting temperature of the corresponding nanoparticles.

Melting temperature (T_m) is a basic physical parameter that has a significant impact on thermodynamic properties. The melting of crystalline materials, as a universal solid−liquid transformation, has been utilized in metallurgy for a long time. Modern systematic studies have provided a relatively clear understanding of melting behaviors, such as surface premelting,[1,2] defect-nucleated microscopic melting mechanisms,[3] and size-dependent T_m of low-dimension materials.[4] Despite the great number of experimental and theoretical studies that have been devoted to understanding melting properties in different kinds of materials, so far this aspect of investigation on polycrystals remains mainly localized to bicrystal models.[5,6]

On a nanometer scale, as a result of elevated surface-to-volume ratio, usually the melting temperatures of metallic particles with a free surface decrease with decreasing of their particle sizes.[7,8] However, recent studies have found that the melting transition for small gallium[9] and tin[10] clusters occurs significantly above their bulk T_m and the size dependence of T_m is not monotonic for sodium clusters in the size range from about 50 to 350 atoms.[11] For the embedded nanoparticles, their melting temperatures may be lower or higher than their corresponding bulk melting temperatures for different matrixes and the epitaxy between the nanoparticles and the embedding matrixes.[12] Nanocrystalline (NC) materials, as an aggregation of nanograins, have a structural characteristic of a very high proportion of grain boundaries (GBs) in contrast to their corresponding conventional microcrystals. As the mean grain size decreases to several nanometers, the atoms in GBs even exceed those in grains, thus, the NC materials can be regarded as composites composed by grains and GBs with a high excess energy. What about the melting behaviors and melting temperatures of NC materials? To the best of our knowledge, there is no report in the literature concerning this subject. The use of large-scale molecular dynamics (MD) simulations has provided an insight into the atomic-scale details on structure and deformation mechanisms of NC materials.[13] In the present paper, we have investigated the size effect on the melting behaviors and the melting temperatures of the infinite NC materials, which is a special case for metallic polycrystals. The atomic-scale details give a clear picture of the melting kinetics in metallic polycrystals.

Because of effects of grain growth, it is invalid to investigate the melting behavior of infinite NC material via continuous heating as widely used in a bicrystal and nanoparticles, etc.,[5−7,14] which indicates basic thermodynamic signature of melting: a discontinuous change in the total energy $E(T)$ as a function of temperature. Because a solid−liquid phase transformation begins to occur at T_m, that is to say, the crystalline materials convert into liquid if the temperature is above T_m, otherwise a remarkable grain growth behavior may be observed in the NC materials, so it is possible to determine the T_m of the NC materials through tentatively varying temperature of the thermostat in MD simulations. It is similar to the solid−liquid coexistence method for determining the T_m of a perfect crystal.[15] This method could be easily implemented in experiment, although it has not been reported in the literature up to now.

The initial atomic configurations of the NC Ag are constructed with a widely used Voronoi cell method.[13] By controlling the distances between each grain center, the numbers of atoms attributed to each grain are approximately uniform, i.e., forming an equal-axis nanocrystal. The stable structures at 0 K are attained through an annealing process of 20 000 MD time steps (40 ps) at 300 K, followed by a cooling procedure with a rate of 50 K/40 ps. All the simulations are carried out under a *NPT* ensemble, except the simulations of nanoparticles under a *NVT* ensemble without period boundary conditions and the interactions between Ag atoms are described with a modified analytic embedded atom method (MAEAM).[16] The MAEAM has been successfully applied in the calculations of surface,[17] nanoparticles,[14,18] and bulk materials.[16] The melting point and the heat of fusion for Ag perfect crystals from MD simulations with the MAEAM potential are 1180 ± 10 K and 9.79 kJ/mol, respectively, which are close to the experimental data of 1234 K and 11.30 kJ/mol. These indicate that the present model for Ag is reliable. The atomic motion equations are integrated with a fourth-order Gear predictor-corrector algorithm and a time step of 2 fs, the temperatures are controlled via a Nose−Hoover thermostat,[19] and the pressures kept at 0 Pa with a Parinello−Rahman scheme.[20] During the determination of melting points,

* Corresponding authors. E-mail: wangyuhu2001cn@yahoo.com.cn (H.W.); shifangxiao@yahoo.com.cn (S.X.).
† Material Science and Engineering College.
‡ Department of Applied Physics.

10.1021/jp054551t CCC: $30.25
Published on Web 10/08/2005

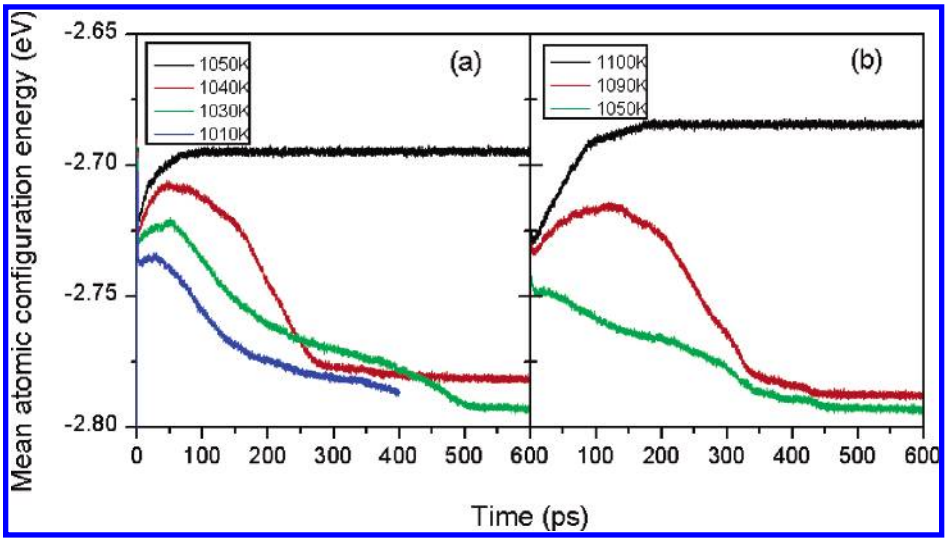

Figure 1. Evolution of the mean atomic configuration energy with relaxation time for specimens with different mean grain size, (a) 3.03 nm, (b) 6.06 nm.

at each temperature, the systems are relaxed 300 000 MD time steps (600 ps), which is sufficient for reaching relaxation equilibrium.

To observe melting evolution, the common neighbor analysis method (CNA)[21] is performed to analyze the atomic local configuration. In this analysis, snapshots of the atomic structure are periodically stored (every 2000 MD time steps), and followed by a steepest-descent path to potential energy minimization,[22] which guarantees that the instantaneous states can be kept and the CNA is not influenced by the thermal fluctuations of the atomic positions.

Figure 1 shows the evolution of the mean atomic configuration energy with heating time for two different specimens around their melting points in MD relaxation processes. There exist two types of characteristic energy−time curves. At the temperature of 1050 K in Figure 1a and 1100 K in Figure 1b, the atomic energy increases continuously until the systems absolutely turn into liquid states. While at the other temperatures ($\leq$1040 K in Figure 1a and $\leq$1090 K in Figure 1b), first, there is a little increment of the atomic energy because of the thermal relaxation starting from stable structure at 0 K, and subsequently, it drops sharply as a result of grain growth. The behavior of melting or grain growth also has been confirmed from the CNA structural analysis and radial distribution function (RDF). Following the common practice as a solid−liquid coexistence simulation, T_m is determined as the temperature at the midpoint of the "melting region", thus the melting points for these specimens shown in Figure 1a and b are 1045 $\pm$ 5 K and 1095 $\pm$ 5 K, respectively.

The grain size dependence of T_m of the NC Ag is shown in Figure 2, and the melting temperatures of the nanoparticles with corresponding size and a fcc crystalline structure are also shown. In comparison to T_m (bulk) = 1180 $\pm$ 10 K simulated from the solid−liquid coexistence method with the present MAEAM potential, the melting temperatures of the NC Ag are slightly below T_m (bulk) and decrease with the reduction of the mean grain size. This behavior can be interpreted as the effects of GBs on the T_m of a polycrystal. MD simulations on a bicrystal model have shown that an interfacial melting transition occurs at a temperature distinctly lower than T_m (bulk) and the width of an interfacial region behaving like a melt grows significantly with temperature.[6] This will induce the grains in a polycrystal melted at a temperature lower than T_m (bulk), when the mean

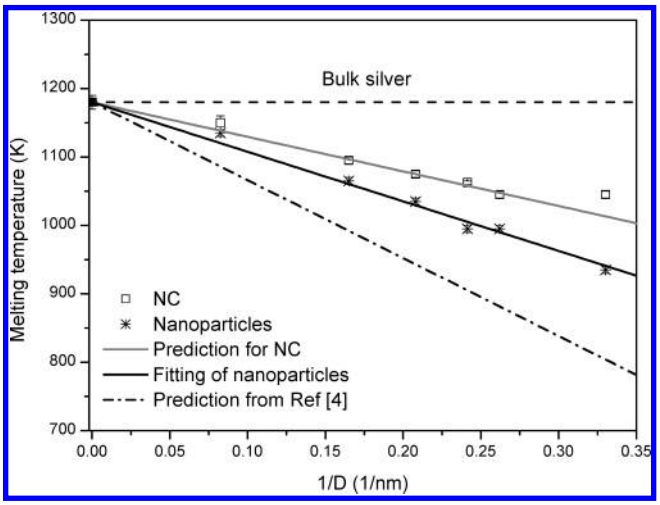

Figure 2. Melting temperatures as a function of the mean grain size for nanocrystalline Ag and of the particle size for the Ag nanoparticle.

grain size decreases to some extent and results in the depression of T_m for the NC materials.

In comparison with the corresponding nanoparticles of the same size, the NC material has a higher T_m. This is to be expected because the atoms on GB are of a larger coordination number than those on a free surface, and the interfacial energy (γ_{GB}) is less than the surface energy (γ_{Sur}). It is well-known that the main difference between the free particles and the embedded particles or grains in a polycrystal is the interfacial atomic structure. A thermodynamic prediction[4] of T_m for free particles was proposed as follows

$$T_m = T_{mb}(1 - (\beta/d)) \quad (1)$$

where T_{mb} is T_m for the conventional crystal, β is a parameter relative to materials, and d is the mean diameter of the grain. By using the suppositions in deducing eq 1, the value of β for Ag obtained from the liquid-drop model[4] is 0.965, and the calculated melting temperatures are shown in Figure 2 as a broken dashed line. The predicted values are much lower than the present simulated data for nanoparticles, and this tendency is the same for several other elements.[23] It is obvious that this value of β from the liquid-drop model is not suitable for prediction of T_m of Ag nanoparticles. Through the linear fitting of the data from the MD simulations for Ag nanoparticles in

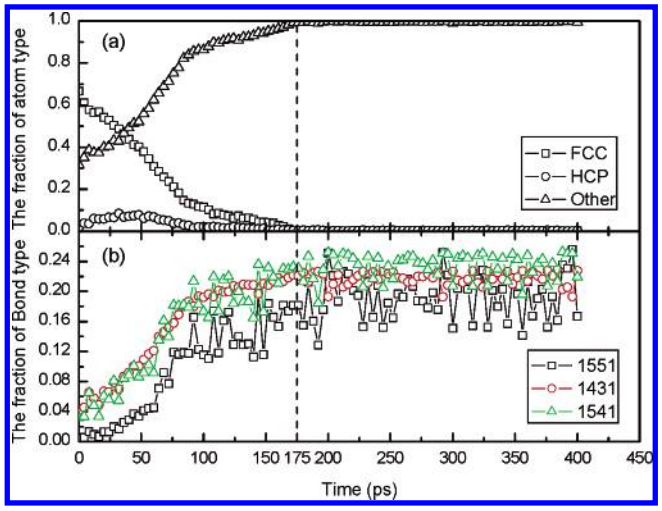

Figure 3. Typical bond type existing in the liquid phase and atom type (from CNA analysis) evolution with MD relaxation time for specimen with a mean grain size of 6.06 nm (T_m: 1095 ± 5 K) at 1100 K.

terms of eq 1, the value of β is determined as 0.614. By considering the difference between the interfacial energy and the surface energy, an expression describing the mean grain size-dependent T_m for NC materials is proposed as follows:

$$T_m = T_{mb}(1 - (\beta/d)(1 - \gamma_{GB}/\gamma_{Sur})) \quad (2)$$

where $\gamma_{GB} = 375.0$ mJ/m^2 (ref 24) and $\gamma_{Sur} = 1240.0$ mJ/m^2 (ref 25) for Ag. On the basis of the fitted value $\beta = 0.614$, the prediction of T_m of the NC Ag from eq 2 gives a good agreement with the values from the MD simulations, as shown in Figure 2. Thus, the melting temperatures of the NC materials can be qualitatively estimated from the melting temperatures of the corresponding nanoparticles. In addition, considering the competitive structural motifs for small nanoclusters, the grain size dependence of T_m for nanoscale materials have little deviation from the proportional relation based on the fcc structural grains, especially at small grain size.

According to the local atomic configurations from the CNA, the atoms are classified into three classes: fcc, hcp, and the others; this makes the evolution of grains and GBs visible during the melting process. Figure 3 shows the relative number of three structural classes of atoms (a) and that of typical bonded pairs existing in metallic liquid (b) as a function of heating time during melting. With the melting developing, the fraction of atoms with a local fcc structure drops rapidly from an initial value of 66.6% to 0 at 175 ps as the NC material turns into a liquid phase completely. On the contrary, the relative numbers of the three typical bonded pairs, (1551), (1431), and (1541), which indicates the liquid (or like liquid) structural characteristics, increase rapidly from 0.4%, 4.1%, and 3.2% to the average values of 19.2%, 21.7%, and 23.3%, respectively, i.e., the fraction of the liquid phase (or like liquid) increases. It reveals that the melting in the polycrystals is a gradual process with heating time. Corresponding to a quantitative description on structural evolution (shown in Figure 3), Figure 4 illustrates the three-dimensional (3D) snapshots of grains in the NC material during melting. It is found that the melting in the polycrystals starts from the GB. Along with melting, the interfacial regions (liquid or like liquid) between grains widen and the grains diminish until they absolutely vanish.

To summarize, a method to determine the T_m of nanocrystalline materials is presented. As a result of smaller-size grains and a larger proportion of GBs with a higher excess energy, the T_m of infinite NC materials decreases with decreasing the mean grain size. In metallic nanocrystalline materials, the melting is a gradual process that starts from the GB regions and evolves toward the interior of grains. The enhancement of the relative numbers of the three typical bonded pairs in a liquid phase gives a good description on kinetic structural evolution in the course of melting.

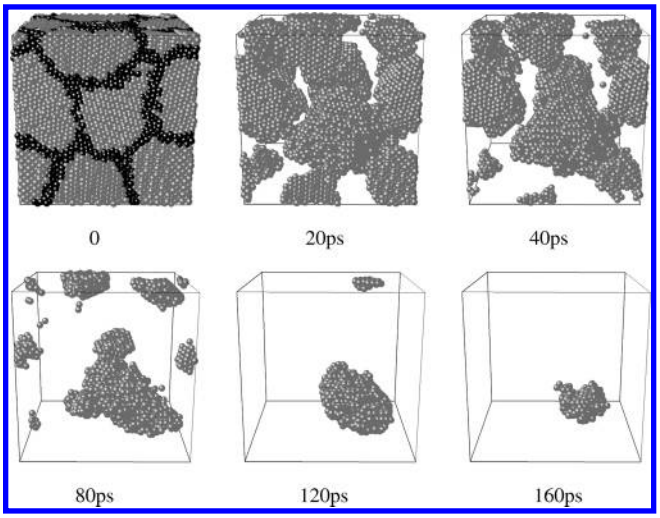

Figure 4. Three-dimensional snapshots of atomic positions in the course of melting for a specimen with a mean grain size of 6.06 nm at 1100 K. The gray spheres denote atoms with a local fcc structure, and the black spheres denote the other type of atoms on GB. For clarity, only fcc atoms are sketched during melting.

Acknowledgment. This work is financially supported by the NSFC (No.50371026), the Hunan Provincial Natural Science Foundation, and the High Performance Computing Center of Hunan University.

References and Notes

(1) Stoltze, P. *J. Chem. Phys.* **1990**, *92*, 6306.
(2) Peters, K. F.; Chung, Y. W.; Cohen, J. B. *Appl. Phys. Lett.* **1997**, *71*, 2391.
(3) Lutsko, J. F.; Wolf, D.; Phillpot, S. R.; Yip, S. *Phys. Rev. B* **1989**, *40*, 2841.
(4) Nanda, K. K.; Sahu, S. N.; Behera, S. N. *Phys. Rev. A* **2002**, *66*, 013208 and the references therein.
(5) Broughton, J. Q.; Gilmer, G. H. *Phys. Rev. Lett.* **1986**, *56*, 2692.
(6) Nguyen, T.; Ho, P. S.; Kwok, T.; Nitta, C.; Yip, S. *Phys. Rev. Lett.* **1986**, *57*, 1919.
(7) Ercolessi, F.; Andreoni, W.; Tosatti, E. *Phys. Rev. Lett.* **1991**, *66*, 911.
(8) Peters, K. F.; Cohen, J. B.; Chung, Y. W. *Phys. Rev. B* **1998**, *57*, 13430.
(9) Breaus, G. A.; Benirschke, R. C.; Suqai, T.; Kinnear, B. S.; Jarrold, M. F. *Phys. Rev. Lett.* **2003**, *91*, 215508.
(10) Shvartsburg, A. A.; Jarrold, M. F. *Phys. Rev. Lett.* **2000**, *85*, 2530.
(11) Aguado, A.; Lopez, J. M. *Phys. Rev. Lett.* **2005**, *94*, 233401.
(12) Sheng, H. W.; Lu, K.; Ma, E. *Nanostruct. Mater.* **1998**, *10*, 865.
(13) Schiotz, J.; Vegge, T.; Di Tolla, F. D.; Jacobsen, K. W. *Phys. Rev. B* **1999**, *60*, 11971.
(14) Hu, W. Y.; Xiao, S. F.; Yang J. Y.; Zhang, Z. *Eur. Phys. J. B* **2005**, *45*, 547.
(15) Morris, J. R.; Wang, C. Z.; Ho, K. M.; Chan, C. T. *Phys. Rev. B* **1994**, *49*, 3109.
(16) Hu W. Y. In *Proceedings of the International Conference on New Frontiers of Process Science and Engineering in Advanced Materials, 14th IKETANI Conference*, Kyoto, Japan, 2004.
(17) Yang, J. Y.; Hu, W. Y.; Deng, H. Q.; Zhao, D. L. *Surf. Sci.* **2004**, *572*, 439.
(18) Zhang, Z.; Hu, W. Y.; Xiao, S. F. *J. Chem. Phys.* **2005**, *122*, 214501.
(19) Nose, S. *J. Phys.: Condens. Matter* **1990**, *2*, 115.
(20) Parrinello, M.; Rahman, A. *J. Appl. Phys.* **1981**, *52*, 7182.

(21) Honeycutt, J. D.; Andersen, H. C. *J. Phys. Chem.* **1987**, *91*, 4950.
(22) Stillinger, F. H.; Weber, T. A. *Phys. Rev. A* **1982**, *25*, 978.
(23) Qi, W. H.; Wang, M. P. *Mater. Chem. Phys.* **2004**, *88*, 280.
(24) Murr, L. E. *Interfacial Phenomena in Metals and Alloys*; Addison-Wesley: New York, 1975.
(25) Tyson, W. R.; Miller, W. A. *Surf. Sci.* **1997**, *62*, 267.